RSC Advances

ROYAL SOCIETY OF CHEMISTRY

www.rsc.org/advances

TOC

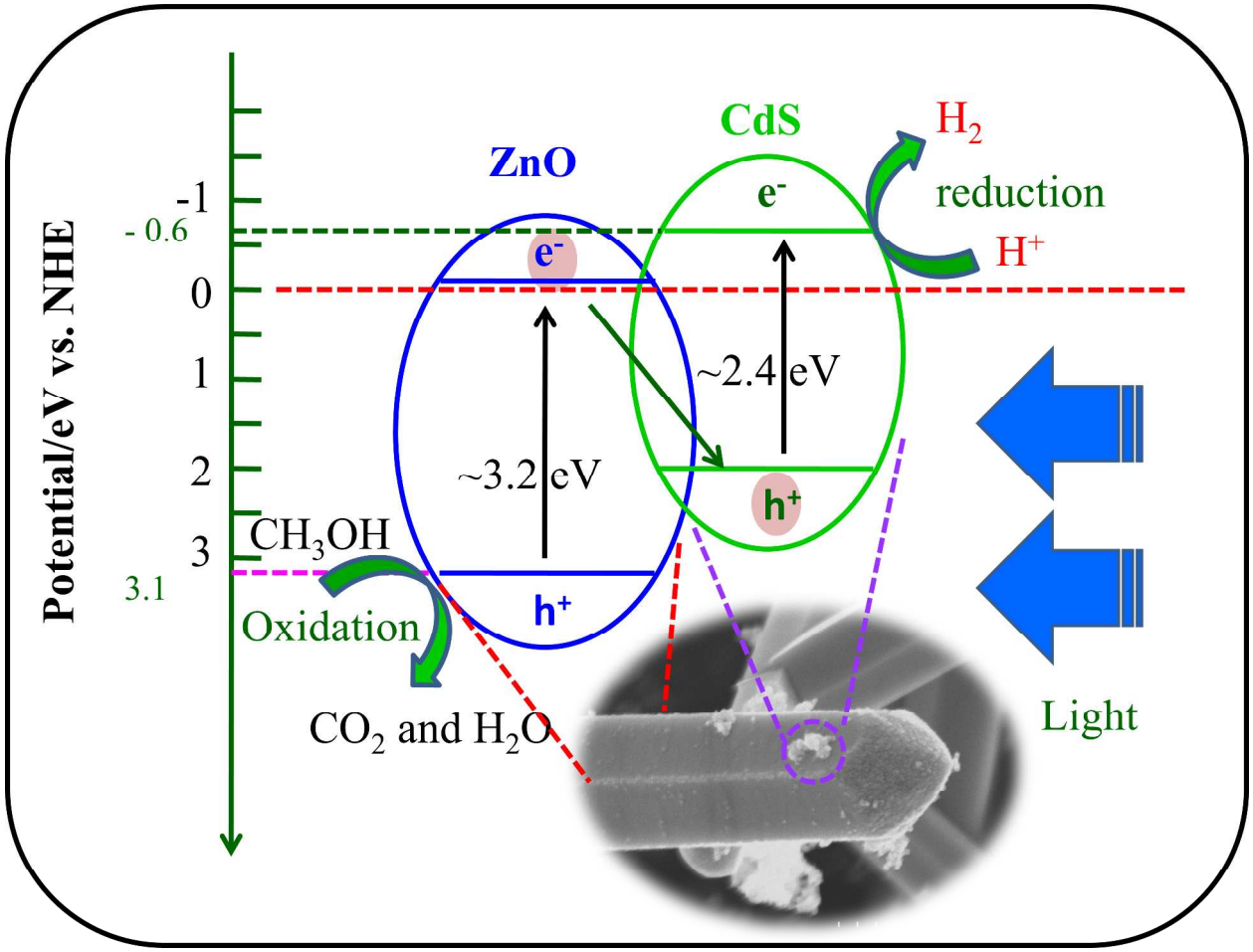

Cite this: DOI: 10.1039/c0xx00000x

www.rsc.org/xxxxxx

ARTICLE TYPE

One Dimensional CdS/ZnO Nanocomposites: An Efficient Photocatalyst for Hydrogen Generation

Jamuna K. Vaishnav, Sudhir S. Arbuj*, Sunit B. Rane and Dinesh P. Amalnerkar

Received (in XXX, XXX) Xth XXXXXXXXX 20XX, Accepted Xth XXXXXXXXX 20XX

DOI: 10.1039/b000000x

One dimensional ZnO nanostructures were synthesized using solvothermal reaction method, and in-situ CdS nanoparticles was grown on 1D ZnO having different CdS compositions such as 0.1, 0.5, 1 and 5 mol% respectively using microwave reaction system. The prepared CdS/ZnO coupled semiconductor catalysts were characterized using various spectroscopic techniques. XRD analysis indicates the presence of wurtzite structure for all the prepared CdS/ZnO compositions. DRS spectrum shows the red shift in the absorbance edge of CdS/ZnO nanocomposites with increase in CdS mol%, absorbance increases in 400 to 500 nm range. Photoluminescence spectra illustrated two emission peaks; first one at 390 nm due to the band edge emission of ZnO and second broad peak centered around 480 nm may be due to CdS band edge emission or oxygen vacancies in ZnO. FESEM image showed formation of pencil shape one dimensional ZnO nanorods containing spherical CdS nanoparticles on the surface of ZnO. TEM analysis confirms the rod like morphology of ZnO and presence of CdS nanoparticles. The activity of prepared CdS/ZnO catalyst was evaluated by measuring the amount of H_2 generated during photocatalytic H_2 evolution from water. The photocatalytic activity of prepared coupled CdS/ZnO shows increase in hydrogen generation as compared to individual ones. The CdS loading enhances the rate of H_2 generation and is the highest for 5 mol% CdS/ZnO composition.

1. Introduction

Conventional energy resources have been depleted to a great extent with continuously rising energy demands. Therefore, it is necessary to find out an alternative economically viable fuel which can fulfil the energy requirements. Hydrogen has been identified as a potential energy carrier in many low greenhouse gases (GHG) energy scenarios. However, the technology to produce hydrogen in a cost-effective, low-GHG manner has not yet been developed.[1, 2] The photocatalytic water splitting under solar light has been considered as one of the most promising technique for renewable hydrogen production.[3] In 1972, Fujishima and Honda achieved ultra violet light induced water cleavage using (TiO_2) photo anode in combination with a platinum counter electrode soaked in an electrolyte aqueous solution, since then enormous amount of efforts were taken to increase the efficiency of photocatalyst for water splitting using artificial or natural sunlight.[4, 5] Up to 1980 enough knowledge has been gained about semiconductor photo-electrochemistry which helped a lot, to develop heterogeneous photocatalysis but still scientific community is in search of highly active photocatalytic system.[6] Till today various semiconductor oxides as well as sulfides have been exploited viz. TiO_2, ZnO, SnO_2, WO_3, Fe_2O_3, Ga_2O_3, CdS, ZnS, SnS_2 and so on, as photocatalyst for energy as well as environment related applications.[7-16] In order to utilize the visible portion of solar spectrum, band gap of the existing wide band gap photocatalysts were lowered by doping cations as well as anions. [17, 18] Also, increase in the photocatalytic activity was observed by loading noble metals on the surface of semiconductors.[19] Furthermore, the change in synthesis methods showed change in the photocatalytic activity as function of surface area and crystallanity. Liu and co-workers utilised the bio-inspired materials for fabricating the hierarchical photocatalyst and observed the enhanced photocatalytic activity.[20-22] Coupled semiconductor systems of oxide/oxide as well as sulphide/oxide type also reported to have enhanced photoactivity.[23-28] Tak and co-workers mentioned the enhanced photocatalytic activities of coupled semiconductors based on two important reasons. First, in the coupled semiconductor systems containing different energy levels, wide band-gap semiconductors can utilize visible light by coupling narrow band-gap semiconductors. Second, charge injection from one semiconductor into another can lead to efficient and longer charge separation by reducing the electron–hole pair recombinations. [29] Apart from metal sulfides and oxides recently use of carbon nanotubes and graphene in combination with TiO_2 and ZnO showed higher photoactivity as compared to their individual activity. [30, 31] CdS is one of the most studied visible light active photocatalyst for H_2 generation via water splitting. [32-34] Recently, many researchers have reported the CdS / ZnO coupled catalytic systems with enhanced activity.[35] Additionally, apart from sulfide/oxide system use of sulfide/sulfide coupled system was also being reported by Zong and co-workers.[36] In this regard herein, we have prepared the CdS/ZnO nanostructured catalytic

system with variation of CdS mol% from 0.1 to 5 and studied their photocatalytic activity towards H_2 evolution reaction.

2. Experimental Section

2.1. Synthesis of one dimensional zinc oxide (1D ZnO)

All chemicals were of analytical grade and used as received without further purification. The chemicals used were zinc acetate (Zn $(CH_3COO)_2$ $2H_2O$), ethylenediammine (EDA, $C_2H_4(NH_2)_2$), sodium hydroxide (NaOH) and methanol (SRL make). For synthesis of 1D ZnO nanorods, 20 mmols of zinc acetate was dissolved in 30 mL methanol. In another beaker 40 mmols of NaOH was dissolved in 20 mL methanol, this solution was added to earlier zinc acetate solution drop wise with constant stirring. After homogeneous mixing 20 mL of EDA was added and stirred for 5 min. Then the resultant mixture was transferred to stainless steel autoclave containing 100 mL teflon container. The autoclave was sealed and kept in an oven at 200 ºC for 24 hrs. After completion of reaction time the autoclave was naturally cooled to room temperature, the formed resultant mass was washed several times with deionised water in order to remove the excess NaOH and EDA. After ensuring the complete removal of EDA and NaOH the material is filtered and dried at 100 ºC for 2 hrs.

2.2. Synthesis of CdS/ZnO nanostructures

For loading CdS nanoparticles on ZnO nanorods with different mol %, 1.5 gm of as synthesized 1D ZnO was taken in four microwave vessel. To these vessel separately prepared solution containing appropriate amount of cadmium nitrate and thiourea in ethylenediammine as a solvent was added and stirred for 10 min. Each vessel contains 1.5 gm of 1D ZnO and stoichiometric amount of Cd, S precursor's viz. 0.1, 0.5, 1 and 5 mol% respectively. After ensuring the homogeneous mixing of ZnO and Cd, S precursors the microwave vessel were set aside in microwave reaction assembly and kept for 30 min at 100 ºC with 300 watt power. After completion of the reaction cycle the material were washed with DI water several times and final wash with ethanol. The obtained CdS/ZnO nanostructures were dried at 50ºC under vacuum, characterized and photocatalytic activity was measured for H_2 generation.

2.3. Photocatalytic H_2 evolution from water

The photocatalytic activity of the prepared CdS/ZnO composites was investigated by measuring the amount of H_2 gas evolved via photocatalytic H_2 evolution from water. For this purpose 100 mL double distilled water was taken in 250 mL round bottom flask, into this 25 mL methanol were added as sacrificial reagent. The 100 mg of CdS/ ZnO composite was added having 1 wt% preloaded platinum as a co-catalyst by photochemical reduction technique. Argon gas was purged through this reaction mixture in order to remove the dissolved oxygen. The 250 mL round bottom flask was connected to the eudiometer tube in order to measure the evolved gas. The eudiometer tube has septum arrangement to remove the evolved gas through gas-tight syringe for quantifying the amount of gases evolved. The whole assembly was kept in a wooden box and the round bottom flask containing reaction mixture was irradiated by 400W mercury vapor lamp. The mercury vapor lamp was fitted in quartz condenser having water circulation arrangement in order to absorb the IR radiation which minimizes the heating effect. As soon as the lamp is switched on, the gases were starts evolving and collected in eudiometer tube. The amount of gas evolved with time were noted and used for the further calculations. The quantification of H_2 gas was carried out using Gas Chromatograph equipped with 5Å capillary column having thermal conductivity detector.

2.4. Characterization

The phases were identified using powder XRD technique (Bruker AXS model D-8, 10 to 70° range, scan rate = 1° min^{-1}) equipped with a monochromator and Ni-filtered Cu Kα radiation. UV-Visible absorbance and diffuse reflectance spectra was recorded using Shimadzu UV-Vis-NIR spectrophotometer (Model UV-3600) over a wavelength range of 200 to 800 nm. The room temperature photoluminescence spectra were obtained from Shimadzu spectrofluorophotometer (RF-5301PC), the excitation wavelength was 350 nm. Time resolved fluorescence spectra were taken on Fluorolog HORIBA Jobin Yvon fluorescence spectrophotometer. Sample films are prepared by drop cast method on quartz plate. The morphological characterization of the samples was performed on HITACHI S-4800. Microstructure analysis were carried out using transmission electron micrograph performed using Technai 20 G2 (FEI, Netherlands) microscope operating at 200kV.

3. Results and discussion

3.1. X-ray diffraction analysis

The synthesized CdS/ZnO nanostructures were characterized using XRD technique in order to investigate the crystalline phase. Fig. 1 depicts the XRD pattern of CdS/ ZnO having different CdS mol% varies from 0.1 to 5 mol %. The XRD peaks observed at 2θ = 31.7, 34.4, 36.2, 47.5, 56.6 and 62.8º corresponds to hkl planes (100), (002), (101), (102), (110) and (200) respectively, which confirms the formation of crystalline ZnO having hexagonal wurtzite phase in all four compositions. The XRD patterns containing sharp and intense peaks are well matches with standard ZnO (JCPDS No. 36-1451).

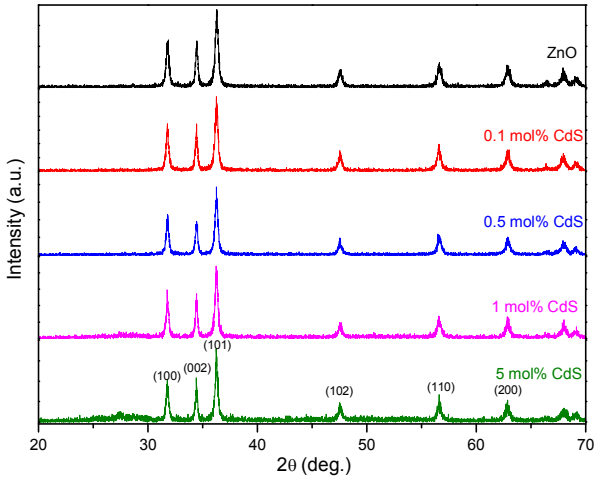

Fig. 1. XRD pattern of pure ZnO and CdS/ZnO nano composites

XRD of pristine ZnO and CdS/ZnO composites were identical, the CdS does not show any individual peak this might be because

of the lower concentration of CdS which is much lower than the XRD detection limit. But in case of 5 mol % CdS/ ZnO very small intensity peak in the range of 24 to 30º are observed which is attributed to hexagonal CdS. The separate XRD of 1 and 5 mol% CdS/ZnO nanocomposites are depicted in supporting information (Fig. S1 and Fig. S2).

3.2. FE-SEM analysis

The FESEM images of CdS/ZnO nanostructures are shown in Fig. 2. Pure ZnO indicates the formation of pencil shaped rod like morphology having length in the range of 4 to 5 µm and diameter around 200 to 300 nm (supporting information Fig. S1). The 0.1 mol% CdS/ZnO shows the presence of spherical CdS nanoparticles on the surface of ZnO rods (Fig.2 a), the size of CdS nanoparticles are in the range of 20 to 30 nm. With further increase in CdS concentration the spherical particles on ZnO surface and also in the form of agglomerated form were seen (Fig. 2b). CdS loaded with 1 mol% retain the same morphology of CdS/ZnO composite, the high and low resolution FE-SEM images indicate the homogeneously distributed CdS on ZnO rods (Fig. 2c, c').

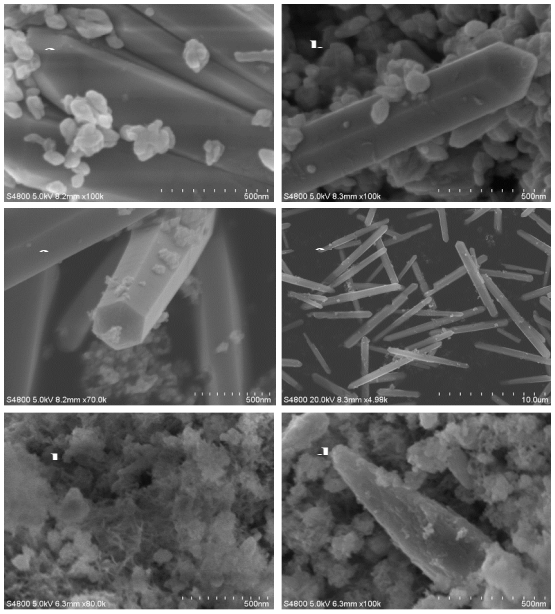

Fig. 2. FESEM of CdS/ZnO nanostructures with varying CdS amount where a) 0.1, b) 0.5, c, c') 1 and d, d') 5 mol %

Further increase in CdS mol% (up to 5%) leads to the formation of CdS nano wires having diameter ~5 nm and length in the range of 50 to 200 nm (Fig. 2d, d'). The CdS nano wire covers the ZnO nanorods, Fig. 2d, d' clearly indicate the presence of CdS wire wrap the ZnO rods forming CdS/ZnO coupled photocatalyst. The solvent plays an important role on the growth of nanoparticles, in the present study solvent used was ethylenediamine (EDA) which is well known structure directing agent.[37] EDA forms a complex with Zn ion and restricts the existence of free zinc ions in solution resulting control formation of zinc nuclei. Further increase in the reaction temperature results decomposition of zinc - EDA complex and form $Zn(OH)_2$. The ZnO formed by decomposition of $Zn(OH)_2$, once the super saturation of ZnO reached the formation of ZnO crystal starts and growth takes place as per crystal habit. Overall, EDA acts as a ligand as well as capping agent and selectively adsorbed on the lateral faces of ZnO nanorods which further inhibits lateral growth.[38] The same phenomenon was observed in case of in-situ CdS loading on ZnO rods, for CdS synthesis the solvent used was EDA and followed the same mechanism of forming Cd-EDA complex. For lower CdS concentrations the particles have spherical shape but in case of higher CdS (5 mol.%) formation of CdS nano wires wrapped on ZnO nanorods were seen. The quantitative estimation of CdS/ZnO mol% were carried out using SEM-EDX analysis and found to be matching almost with the experimental values.

3.3. TEM analysis

TEM images of CdS/ZnO coupled catalyst are shown in Fig. 3. CdS/ZnO nanocomposites with 0.1 and 0.5 mol% CdS validate the presence of spherical CdS nanoparticles on the surface of ZnO nanorods (Fig. 3 a, b). The size of CdS nanoparticles are *ca* 20 nm, and observed to be present on the surface of ZnO nanorods as well as separately in agglomerated form.

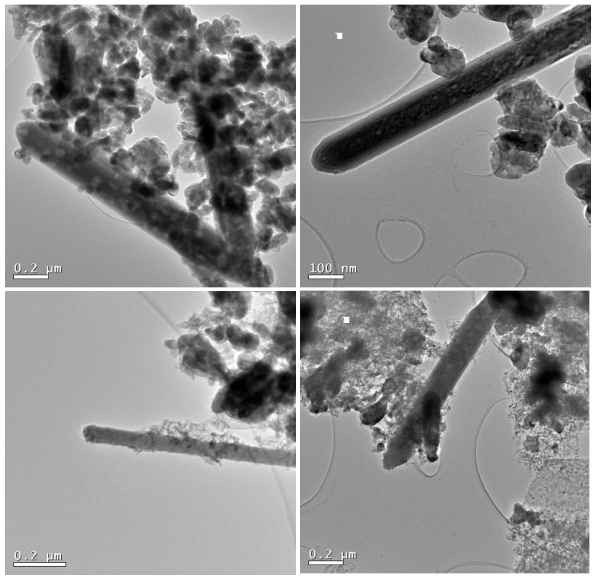

Fig.3 TEM of CdS/ZnO nanostructures with varying CdS amount where a) 0.1, b) 0.5, c) 1 and d) 5 mol %

With higher CdS loading the formation of CdS nano wire wrapped on ZnO rods were evident from the TEM analysis (Fig.3 c, d). Overall the presence of CdS on ZnO nano rods in the prepared CdS/ZnO compositions was confirmed by TEM analysis.

3.4. Optical study

3.4.1. Diffuse reflectance UV-Visible absorbance spectra (DRS)

The diffuse reflectance spectra of 1D CdS/ZnO nanostructures for all prepared compositions are shown in Fig. 4. The absorption band edge of pure ZnO is observed at 390 nm corresponds to 3.18 eV. With increase in CdS concentration in CdS/ZnO composites the absorption edge shows red shift, the absorbance increases in the range of 400 to 500 nm. This improved absorbance in the visible region was due to the presence of CdS nanostructures and

also absorbance edge of CdS/ZnO composites shift from 390 to 500 nm respectively. The red shift in DRS spectra indicates the presence of CdS in CdS/ZnO composites.

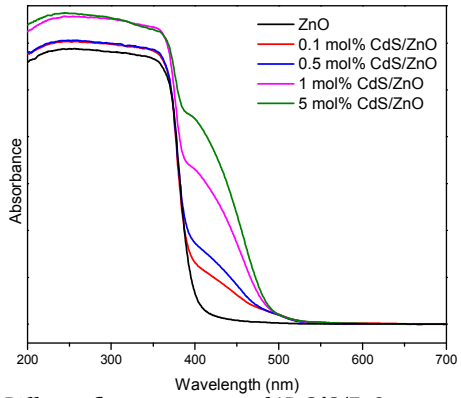

Fig. 4 Diffuse reflectance spectra of 1D CdS/ZnO nanocomposites

Furthermore the presence of hump at 400 nm in all the compositions validates the existence of separate phases of CdS and ZnO. DRS pattern confirm the formation of coupled CdS/ZnO catalyst which is already validated from TEM analysis.

3.4.2. Photoluminescence spectra (PL)

The room-temperature PL spectra of typical 1D CdS/ZnO composites were obtained with an excitation wavelength of 350 nm and are shown in Fig. 5. Pure ZnO as well as CdS/ZnO composites showed two distinct peaks at 390 and 500 nm. The sharp and intense ultra violet emission peak at 390 nm is attributed due to the band gap excitation and the broad emission peak centered at 500 nm observed due to oxygen vacancies in ZnO lattice. The intensity of peak at 390 nm goes on decreasing with increase in CdS mol %, this might be due to wrapping of ZnO with CdS nanoparticles which lowers the effective area for the photon absorption, secondly the quenching of PL may takes place due to transfer of photogenerated conduction band electrons.

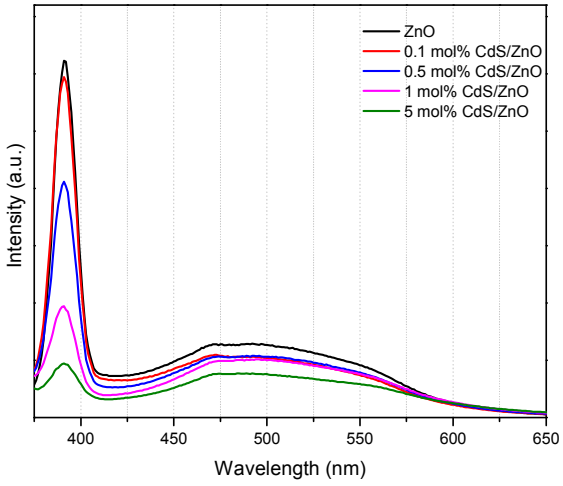

Fig. 5 Photoluminescence spectra of 1D CdS/ZnO nanocomposites

Additionally, the presence of broad green emission band centered at 500 nm that lies in the visible region generally nominated as deep level emission (DLE) is probably related to the variation of intrinsic defects in ZnO, such as zinc vacancy, oxygen vacancy, interstitial zinc, interstitial oxygen and antisite oxygen. In a word, the origin of the visible emission in ZnO is highly controversial.[39] The *Pol et al* reported green emission is due to the recombination of the electrons in singly ionized oxygen vacancies and the recombination of a photogenerated hole with a single ionized charge state of the specific defects (oxygen vacancies and Zn interstitials).[40]

3.5. Photocatalytic activity study

After complete structural characterization of the material, photocatalytic activity of 1D CdS/ZnO composites were evaluated by measuring the amount of H_2 produced through photocatalytic H_2 evolution reaction. The graph of amount of H_2 produced Vs irradiation time for different compositions of 1D CdS/ZnO coupled catalyst are shown in Fig. 6. The pure CdS and ZnO shows 445 and 300 µmoles of H_2 after 4 hrs of irradiation respectively, This lower activity is because of the band gap of ZnO is 3.18 eV and it absorb only UV light and not the visible light which leads the lower number of electron-hole pair generation resulting poor activity. As the amount of CdS loading increases the H_2 evolution also increases. The 5 mol% CdS/ZnO composite showed highest amount of H_2 evolution (647 µmoles/0.1 gm) among the other prepared compositions within four hours of irradiation.

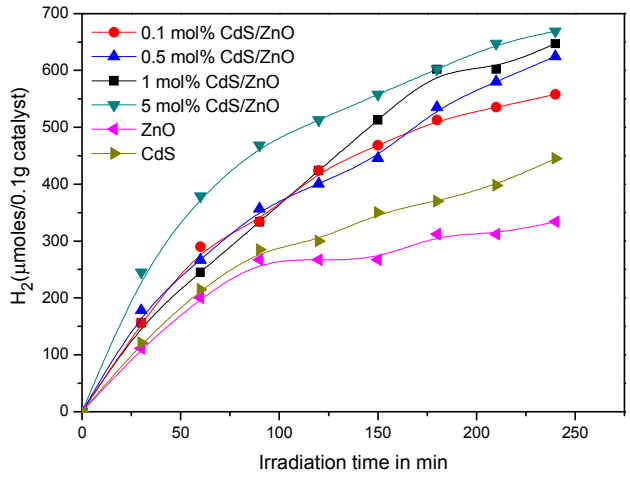

Fig. 6 Photocatalytic H_2 generation using CdS/ZnO composites

The detail photocatalytic H_2 evolution reaction mechanism is shown in Fig. 7. Upon illumination with light both the materials ZnO as well as CdS absorbs the photons and creates respective electron-hole pairs by means of transferring valence band electron to the conduction band. It is well reported that in coupled semiconductor system the photocatalytic activity is higher due to lowering of recombination rate of formed electrons and holes. In the present study of CdS/ZnO nanocomposites, the CdS and ZnO absorb visible (< ~515 nm) and (< ~ 390 nm) UV light respectively. The conduction band of CdS is more negative as compared to ZnO than the H_2 evolution potential.[41] As the CdS mole ratio increase in CdS/ZnO composites the CdS absorb in the visible region, resulting increase in the absorbance wavelength range. This enhanced absorbance leads to the formation of more number of electron- hole pairs resulting higher photocatalytic activity. The enhanced photocatalytic activity has two possible mechanisms on the basis of recombination of conduction band

(CB) electrons and valence band (VB) holes formed in CdS and ZnO. a) The CB electron from ZnO combines with VB hole of CdS (Fig. 7). And remaining CB electron in CdS was captured by Pt co-catalyst for further reaction to generate H_2 gas, mean while VB hole in ZnO react with methanol to produce CO_2 and H_2O.

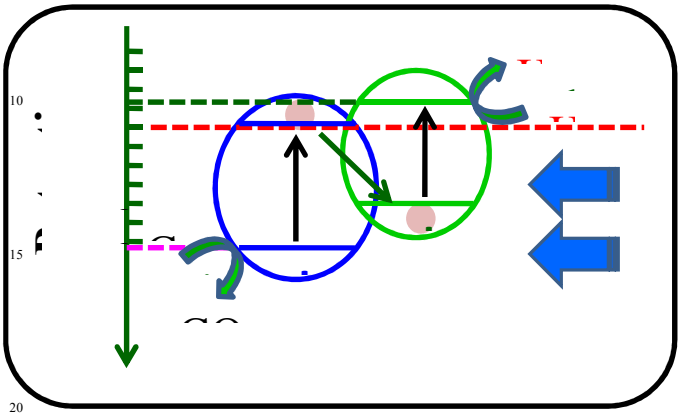

Fig. 7 Schematic band structures of CdS/ZnO nanocomposites for H_2 evolution reaction

Cheng and co-workers suggested the same mechanism on the basis of fluorescence emission decay spectra of ZnO/CdS hetero structure. [42] b) In another mechanism, CdS absorb the photon having appropriate wavelength and generates electron-hole pairs. The conduction band electron of CdS transfer to the conduction band of ZnO where the H^+ ions get reduced to form H_2 gas. In both the cases the rate of recombination of electron-hole pairs was lowered resulting higher activity. This phenomenon is responsible for higher activity of 5 mol% CdS/ZnO composites.

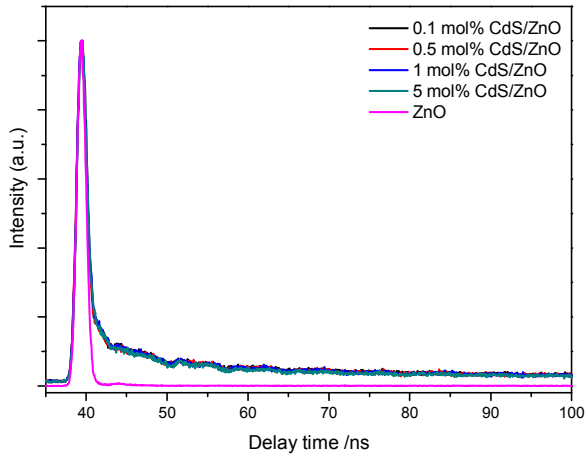

Fig. 8 Time-resolved fluorescence emission decay spectra of ZnO and CdS/ZnO nanocomposites

To support our mechanism (Fig. 7) we studied the decay behaviour of prepared CdS/ZnO nanocomposites using time-resolved fluorescence study. The electron decay behaviour can also be studied using time-resolved mid-IR absorption spectroscopy. Li and co-workers studied the kinetics of photogenerated electrons in Zn and Pb-doped β-Ga_2O_3.[43] The fluorescence emission decay spectra are shown in Fig. 8. The decay life time of carries in pure ZnO is around 41 ns, while that of prepared CdS/ZnO nanocomposites have *ca* 90 ns. This supports our investigation of transferring of photo-excited electrons and holes between CdS and ZnO, which minimises the recombination and improve the photocatalytic activity of nanocomposites. In a word, CdS/ZnO nanostructures facilitate the charge separation, resulting in the generation of long-lived electron-hole pairs.

4. Conclusions

The 1D CdS/ZnO coupled catalyst with different CdS mole ratios were prepared using microwave assisted semi-solvothermal technique. XRD validate the formation of hexagonal ZnO for all the prepared compositions and peaks due to CdS were not observed as it is below the detectable range of XRD. The DRS spectra of CdS/ZnO composites indicate the red shift in the absorbance spectra due to presence of CdS nanostructures. The prepared catalyst utilizes the visible portion of light which would be beneficial for enhancement of photocatalytic activity. Lowering of PL emission peak intensity with increase in CdS mol% indicates the formation of coupled catalytic system, the lowering of intensity may be due to the electron transfer among the conduction band of CdS and ZnO. FESEM and TEM analysis confirms the formation of rod like morphology having CdS nanoparticles on the surface of ZnO rods. For higher CdS mol% nano wire wrapping ZnO rods was observed as the used EDA acts as structure directing agent. The activity of prepared coupled CdS/ZnO catalyst shows improved hydrogen generation via photocatalytic H_2 evolution from water, the activity increases with increase in CdS mol%. The enhanced photocatalytic activity was due to wide absorbance spectra of prepared catalyst and secondly lowering of electron-hole recombination process due to couple catalytic system.

Acknowledgement

Authors are grateful to Department of Electronics and Information Technology (DeitY), Govt. of India, New Delhi for financial assistance. Authors are also thankful to Dr. U. P. Mulik, Ex Director, C-MET, and Dr. B. B. Kale, Director, C-MET Pune, for useful discussions and spectroscopic analysis.

Notes and references

Centre for Materials for Electronics Technology, Off Pashan Road, Panchvati,Pune-411008,India, Tel:+91 20 25899273: Fax: +91 20 25898180, E-mail: sudhir1305@gmail.com

1. L. Barreto A. Makihira, K. Riahi Intern. *J. Hydrogen Energy*, 2003, **28**, 267.
2. J. Ogden. *Annu Rev Energy Environ*., 1999, **24**, 227.
3. X. Chen, S. Shen, L. Guo, and S. S. Mao , *Chem. Rev.*, 2010, **110** , 6503.
4. A. Fujishima and K. Honda, *Nature*, 1972, **238**, 37.
5. K. Maeda and K. Domen, *J. Phys. Chem. Lett.*, 2010, **1** , 2655.
6. M. R. Hoffmann, S. T. Martin, W. Choi, D. W. Bahnemann, *Chem. Rev.*, 1995**, 95**, 69.
7. J. Wang, H. Sun, J. Huang, Q. Li, and J. Yang, *J. Phys. Chem. C*, 2014, **118**, 7451.
8. S. S. Arbuj, R. R. Hawaldar, U. P. Mulik, B.N. Wani, D. P. Amalnerkar, S. B. Waghmode, *Mater. Sci. Eng., B* 2010, **168**, 90.
9. S. S. Arbuj, N. Rumale, A. Pokle, J. D. Ambekar, S. B. Rane, U. P. Mulik and D. P. Amalnerkar, *Sci. Adv. Mater.,* 2014, **6**, 269.
10. M. Trejo, P. Santiago, H. Sobral, L. Rendón and U. Pal, *Cryst. Growth Des.*, 2009, **9**, 3024
11. U. Pal, M. Pal, R. S. Zeferino, *J Nanopart Res.,* 2012, **14**, 969.

12. A. Tanaka, K. Hashimoto, and H. Kominami, *J. Am. Chem. Soc.*, 2014, **136**, 586.
13. G. K. Pradhan, D. K. Padhi, and K. M. Parida, *ACS Appl. Mater. Interfaces*, 2013, **5**, 9101.
14. M. G. Ju, X. Wang, W. Z. Liang, Y. Zhao and Can Li, *J. Mater. Chem. A,* 2014, Accepted manuscript, DOI**:** 10.1039/C4TA03193H
15. S. S. Arbuj, S. R. Bhalerao, S. B. Rane, N. Y. Hebalkar, U. P. Mulik and D. P. Amalnerkar, *Nanosci. Nanotechnol. Lett.,* 2013**, 5***,* 1245.
16. J. M. Mali, S. S. Arbuj, J. D. Ambekar, S. B. Rane, U. P. Mulik and D. P. Amalnerkar, *Sci. Adv. Mater***.** 2013, **5***,* 1994.
17. M. Yoshida, K. Maeda, D. Lu, J. Kubota, and K. Domen, *J. Phys. Chem. C*, 2013, **117** 14000.
18. D. Dvoranova, V. Brezova, M. Mazur, M. Malati, *App. Catal.B: Environ.,* 2002, **37**, 91.
19. K. Maeda, K. Teramura, D. Lu, N. Saito, Y. Inoue, and K. Domen, *Angew. Chem*., 2006, **118**, 7970.
20. J. Liu, and M. Antonietti, *Energy Environ. Sci*., 2013, **6**, 1486
21. J. Liu, Q. Yang, W. Yang, M. Li, and Y. Song, *J. Mater. Chem. A*, 2013, **1**, 7760
22. J. Liu, J. Huang, D. Dontosova and M. Antonietti, *RSC Adv*., 2013, **3**, 22988.
23. H. G. Kim, P. H. Borse, W. Choi, and J. S. Lee, *Angew. Chem. Int. Ed*. 2005, **44**, 4585.
24. X. Wang, Q. Xu, M. Li, S. Shen, X. Wang, Y. Wang, Z. Feng, J. Shi, H. Han, and C. Li, *Angew. Chem. Int. Ed*. 2012, **51**, 13089.
25. S. S. Arbuj, U. P. Mulik and D. P. Amalnerkar, *Nanosci. Nanotechnol. Lett.,* 2013, **5**, 968.
26. D. Barpuzary, Z. Khan, N. Vinothkumar, M. De, and M. Qureshi, *J. Phys. Chem. C*, 2012, *116* , 150.
27. L. Nasi , D. Calestani , T. Besagni , P. Ferro , F. Fabbri , F. Licci , and R. Mosca, *J. Phys. Chem. C*, 2012, *116* , 6960.
28. L. Mao, Y. Wang, Y. Zhong, J. Ning and Y. Hu *J. Mater. Chem. A*, 2013,**1**, 8101.
29. Y. Tak, H. Kim, D. Lee and K. Yong, *Chem. Commun*., 2008, 4585.
30. K. Woan, G. Pyrgiotakis and W. Sigmund, *Advanced Mater*. 2009, **21**, 2233.
31. Q. Xiang, J. Yu and M. Jaroniec, *Chem. Soc. Rev.*, 2012, **41**, 782.
32. L. A. Silva, S. Y. Ryu, J. Choi, W. Choi and M. R. Hoffmann, *J. Phys. Chem. C*, 2008, **112**, 12069.
33. Y. Wang, Y. Wang, and R. Xu , *J. Phys. Chem. C*, 2013, **117**, 783.
34. Q. Li, B. Guo, J. Yu, J. Ran, B. Zhang, H. Yan, and J. R. Gong, *J. Am. Chem. Soc.,* 2011, **133**, 10878.
35. D. Barpuzary and M. Qureshi, *ACS Applied Materials & Interfaces,* 2013, **5**, 11673.
36. X. Zong, J. Han, G. Ma, H. Yan, G. Wu, and Can Li *J. Phys. Chem. C*, 2011, **115***,* 12202.
37. D. Xu, Z. Liu, J. Liang, and Y. Qian, *J. Phys. Chem. B*, 2005, 109, 14344.
38. B. Liu, H. C. Zeng, *J. Am. Chem. Soc*., 2003, 125, 4430.
39. K. Vanheusden, C. H. Seager, W. L. Warren, D. R. Tallant, and J. A. Voigt, *J. Appl. Phys*. 1996, **79**, 7983.
40. V. G. Pol, J. M. Calderon-Moreno, and P. Thiyagarajan, *Langmuir,* 2008, **24**, 13640.
41. M. Gratzel, *Nature*, 2001, *414*, 338.
42. X. Wang, G. Liu, Z. G. Chen, F. Li, L. Wang, G. Q. Lu and H. M. Cheng, *Chem. Commun*., 2009, 3452.
43. X. Wang, S. Shen, S. Jin, J. Yang, M. Li, X. Wang, H. Han and C. Li, *Phys. Chem.Chem. Phys*., 2013, *15*, 19380.